Hindawi
International Journal of Photoenergy
Volume 2022, Article ID 7715214, 14 pages
https://doi.org/10.1155/2022/7715214

Research Article

Experimental Investigation and Comparison of the Net Energy Yield Using Control-Based Solar Tracking Systems

Ibrahim Sufian Osman, Ibrahim Khalil Almadani, Nasir Ghazi Hariri, and Taher Saleh Maatallah

Department of Mechanical and Energy Engineering, College of Engineering, Imam Abdulrahman Bin Faisal University, P. O. Box 1982, Dammam 31441, Saudi Arabia

Correspondence should be addressed to Ibrahim Sufian Osman; ibrahim-sufian@hotmail.com

Received 28 March 2022; Accepted 6 June 2022; Published 18 June 2022

Academic Editor: Hafiz Muhammad Ali

As the world trend is going towards renewable energy, solar photovoltaic (PV) energy shines the most due to the low generation cost especially by using the latest PV cell technologies and materials, although the conventional silicon cell has an efficiency in the range of 15-16%. A PV tracking system (PVTS) could be a considerable method to increase electrical PV efficiency. In this study, the performance enhancement of the daily output power and energy has been experimentally investigated using single- and dual-axis tracking mechanisms for flat-plate conventional PV panels under the insolation conditions of the Eastern province of Saudi Arabia (SA). In the current study, the active PVTS has been designed and implemented with PID controllers and controlled in real-time with an embedded system. The fixed-tilt (FTPV), single-axis solar tracking system (SAST), and dual-axis solar tracking system (DAST) were tested simultaneously under clear-sky conditions. The PV electrical energy balance has revealed that the energy consumed by the electrical controllers of the SAST and DAST is 3.4% and 3.9%, respectively. In addition, the energy losses due to the actuators of the SAST and DAST are 7.8% and 13.0%, respectively, where they contributed mainly to the energy losses. However, the PV energy production by the DAST was high enough to compensate for the higher actuating mechanism losing rate compared to the SAST and performed incremental net energy output of around 8.64%. On other hand, the DAST and SAST were more efficient than the FTPV recording higher net energy increase by 28.98% and 18.73%, respectively.

1. Introduction

As the human population grew alongside technology, the energy demand increased rapidly day after another, which led to the industrial revolution at the end of the 19th century, causing a vast consumption of fossil fuel. Although it is a dependable energy source, it has many drawbacks such as greenhouse gas emissions, transportation adversity, and exhaustibility [1–3]. Due to these flaws, in the last decade, renewable energy sources like wind, solar, and geothermal became relevant as they are infinite and most importantly eco-friendly [1–4].

Solar energy is the most used and promising renewable energy source since solar energy technologies have shown considerable improvements in performance and reduction in cost in the past few years [5, 6]. In addition, the annual energy potential received from the sun is approximately 8000 times more than the average energy usage of the whole world [7]. There are three main solar systems: photovoltaic (PV) system, solar thermal system, and hybrid system [8], where a photovoltaic system produces electrical energy, a solar thermal system produces thermal energy, and a hybrid system produces both electric and thermal energy [9]. Recently, energy generated from PV systems became dominant in the market considering that it is noise-free, highly efficient, and inexpensive in production and maintenance costs [3, 10, 11].

Overall, the efficiency of a PV system is affected by many factors, including environmental conditions, such as the PV cell temperature, the amount of solar irradiance, and soiling effect [12–15]. One approach to enhance the overall efficiency of a PV system is by increasing the amount of solar

irradiance that the system receives [12, 14]. The amount of solar irradiance depends significantly on the angle between the sun rays and the normal of the module (incidence angle), so as long as the panel is fixed, it can only receive the maximum amount of irradiance when the sun is perpendicular to the module's surface. Thus, a PVTS tends to improve the PV system efficiency via detecting the direction of the sun rays and adjusting the orientation of the PV module to minimize the incidence angle [16–18].

Solar tracking systems (STS) have three main categories: solar trackers based on driving technique, solar trackers based on movement degree of freedom, and solar trackers based on control method [9]. The first category is solar trackers based on driving techniques with two main types of driving techniques: passive STS and active STS [5, 19, 20]. The second category is solar trackers based on the degree of freedom of the motion, which in general are divided into two subcategories, single-axis solar tracking systems (SAST) and dual-axis solar tracking systems (DAST) [21, 22]. The third category is solar trackers based on the control method, and they have three primal types of control scheme, open-loop, closed-loop, and hybrid (combined) control systems [9, 23, 24]. Various control algorithms can be implemented in solar tracking (ST) techniques, for example, simple on-off, PID, fuzzy, and LQR controllers [25–28]. [29] states that the on-off, fuzzy, and PID controllers are the most used controllers with a utilization percentage of 57.02%, 10.53%, and 6.14% of STS, respectively, while 26.31% of STS are other types of control algorithms. Although all these controllers are used to optimize the PV system power consumption, there are still some concerns regarding the ST technology, such as shading effect, performance under different weather conditions or different regions, initial cost, and maintenance cost.

da Rocha Queiroz, J. et al. [22] assembled a DAST based on Arduino integrated development environment in process language. The DAST has shown a 67.28% total gain and 63.22% net gain while on a cloudy day the total gain was 37.84% and the net gain was equal to 28.99%. In the case of a rainy day, 11.71% total gain is recorded and 19.47% loss. That shows the effect of different weather conditions on the DAST PV system, even though the DAST shows a performance improvement when appropriately applied.

Du, X. et al. [30] highlighted that DAST technology fabrication cost is almost 40% of the total cost of the whole PV system. Furthermore, DAST with an active driving technique consumes more energy than SAST to alter its position regarding the sun since it usually consists of two motors that might consume more power than gained, causing the net efficiency to drop. The cost of the DAST may lead to a greater economic-friendly alternative, and that is the SAST.

Ngo, X. C. et al. [31] studied the efficiency of the SAST in Vietnam (Quang Tri Province) while considering the tracking system energy consumption on different weather conditions. The performance on a sunny day showed an increase of 33.3% in energy generation and an efficiency increase of about 30.3%. While on a cloudy day, a huge efficiency drop accrues compared to a sunny day, where the net increase in efficiency is measured to be 3.2%. The worst-case scenario is when it is rainy; although there is a power generation difference of 6.7%, the net efficiency drops to about -2% since the power consumed via the tracking is more than the energy gained by the solar system itself.

Ruelas, J. et al. [32] made a low-cost PV SAST by using the efficiency as a function of time technique (EFO) at Mexico (Cd. Obregón). The prototype was designed with specific parameters to maintain the cost of production and maintenance low, while its working principle is based on three-point motion control with azimuth angles of 30°, 90°, and 120°. It was found that the system achieved an increase in the collection efficiency of about 24% and a price of 27% lower than the traditional commercial trackers. It is noticeable that the STS has different outcomes depending on the weather conditions of where it is installed, which needs to be further studied.

Eldin, S. A. S. et al. [16] studied the effects of extreme exposure to solar irradiance and how it affects the PVTS temperature and performance. The results of the study showed a 39% gain in electrical energy in a cold environment (Berlin, Germany). On the other hand, results of the same PV STS in the hot environment (Aswan, Egypt) showed an electrical energy gain that does not exceed 8%. The study concludes that the energy consumption from the tracking system was considerable, where the tracking system would not be as useful in hot weather areas as it is in cold weather areas.

In the literature, few studies were conducted in the Arab Gulf countries regarding the feasibility of STS, and most of them are simulation-based ones. In effect, [33] studied the effect of different STS configurations and adjustment periods on the power production in the western region of Saudi Arabia (in Makkah city, SA). The simulation study found that the DAST and SAST produced 34% and 20% power more than the FTPV, respectively. Similarly, [34] investigated the effect of STS on multiple performance indicators in 32 sites in SA. The simulation-based results concluded that DAST is an infeasible choice for the region from an economical point of view, since the difference in energy production between SAST and DAST is only 3-4.5%, and SAST produces 28-33% energy more than the FTPV. Another simulation work was elaborated by [35] in Kuwait, and it was found that using SAST and DAST, the annual energy yield could be increased by 24.7% and 29%, respectively. Furthermore, [36] experimentally carried out a study in order to optimize and investigate the performance of SAST in Bahrain using a micro-controller-based system. The optimized STS has shown that the energy yield might be increased up to 40% compared to FTPV using the proposed STS. [37] compared the experimental average power production of the FTPV and STS systems against their simulation results using the local weather conditions of the United Arab Emirates (UAE). The obtained results showed that there is an increase in the output power of the PV modules of 17.28% compared to FTPV by using an azimuthal STS. The simulation results showed a good agreement with the experimental ones, and the mean relative error was about 2.7%. Moreover, another work was conducted in UAE [38] to evaluate the rate of output power increment that can be achieved by

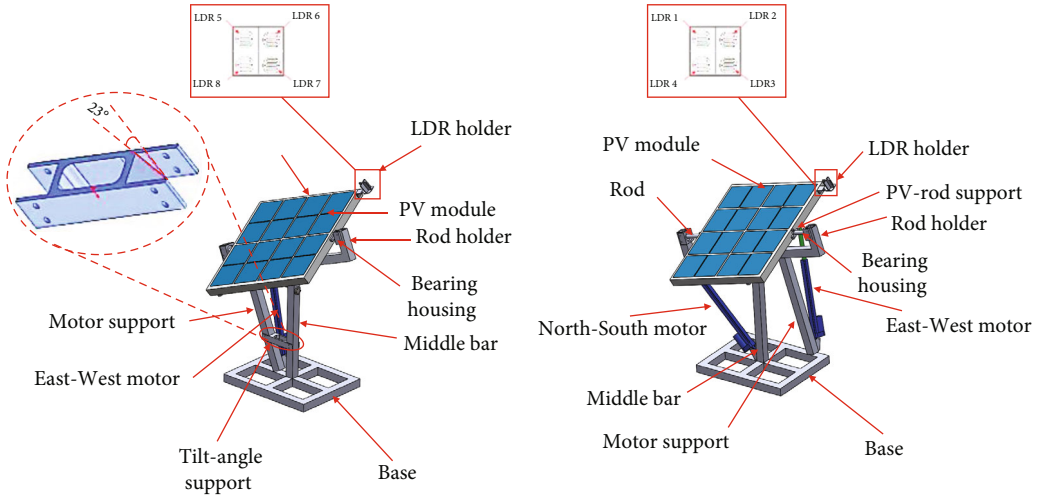

Figure 1: (a) SAST and (b) DAST CAD models.

Table 1: The electrical setup for the experiment.

Component	Model	Specification	Qty
Current sensor	ASC712	Input: 5 V Frequency: 80 kHz Sensitivity: 185 mV/A Error: 1.5%	6
Motor driver	L298N	Input: 12 V Operating current: 0-36 mA Peak current: 2 A	2
Secure digital (SD)	SDHC	Input: 5 V Operating current: 0.2-200 mA	2
Real-time clock (RTC)	DS3231	Input: 5 V Frequency: 100 kHz	1
Power resistor	JIANXIN-09-13-318-02	Power rating: 100 W Resistance value: 8 Ω Tolerance: 5%	3
On/off switch	—	Rating: 3A/6A 250 V Electrical life: 10^3 cycles	1
LDR	—	Input: 5 V	6
Arduino Mega	ATmega2560	Input: 12 V Frequency: 16 MHz	1
Linear motor	—	Input: 12 V Max. speed: 20 mm/s	3
PV module	—	Pmax = 54.2 W Imax = 3.28 W Vmax = 16.54 W Efficiency = 14.24 W	3
Battery	—	Capacity: 100 Ah	1

integrating the STS to a PV panel and Fresnel linear concentrating system. The simulation results revealed that tracking the sun-azimuth can increase the electrical output power by 14.8% and 15.3% compared to the FTPV panel and linear PV concentrator, respectively. Finally, [39] designed a cheap, high-accuracy, and closed-loop DAST using a sun position algorithm with the aim of studying the feasibility of the system in Qatar. The results demonstrated that using such a system may lead to an increase in the PV power generation by 13.9% with respect to the FTPV.

In all the studies mentioned above, researchers have carried on the gain in instantaneous and integrated power yields over a typical measurement time frame that was made by solar tracking mechanisms with respect to FTPV.

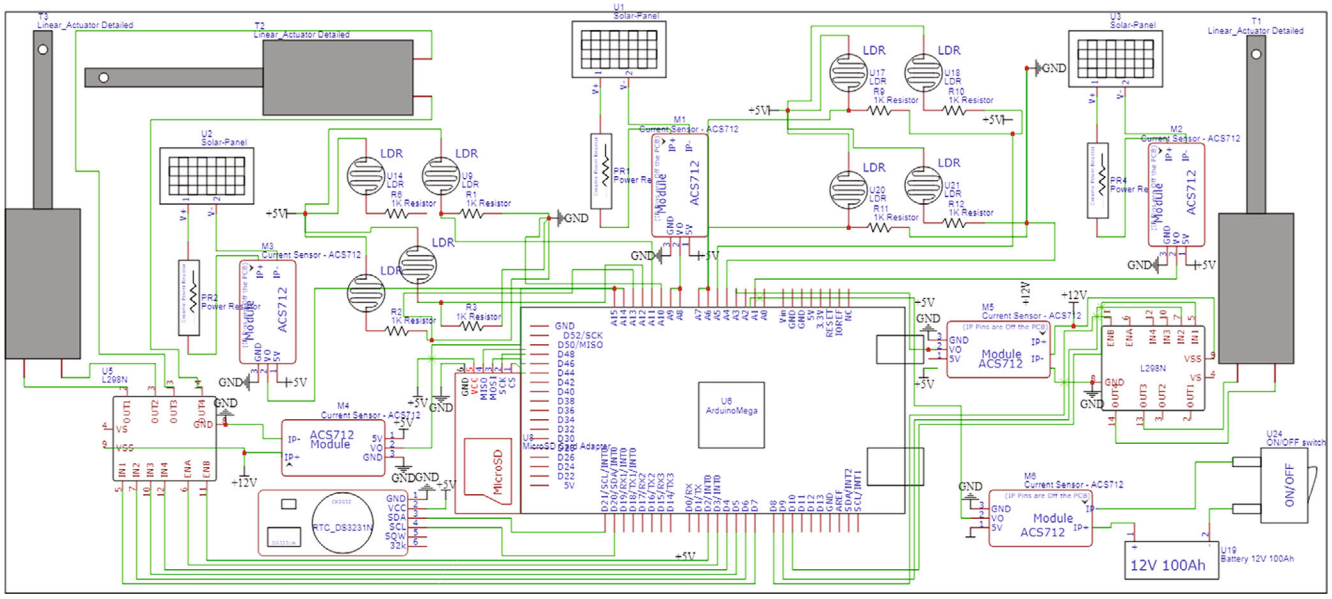

Figure 2: The electrical schematic diagram for the FTPV, SAST, and DAST.

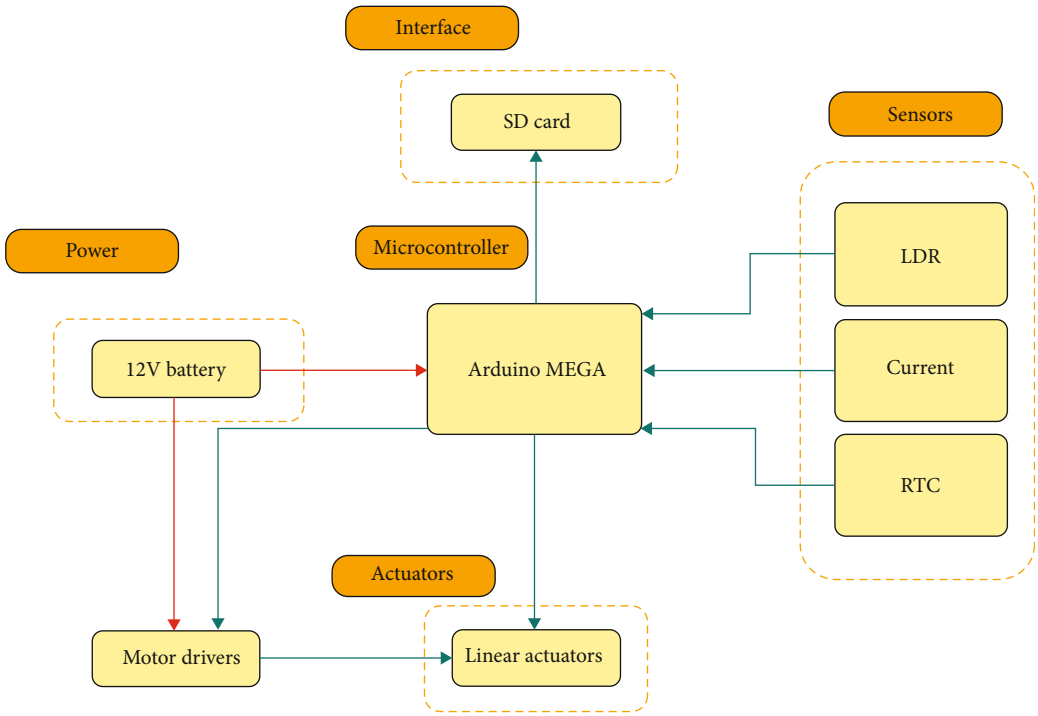

Figure 3: Electrical block diagram for SAST and DAST.

However, the contribution of the actuators and particularly the controllers in the energy consumption and therefore the net output power of the tracked flat-plate PV panels have never been analyzed and discussed in detail. Furthermore, the improvement rates in power and energy of the tracking systems have neither been numerically nor experimentally investigated under the local weather conditions. This is because no previous research studies have experimentally analyzed the net electrical energy of a self-consumption fixed or tracked PV panel under the Saudi environmental conditions and more particularly of Dammam city (26°26′03″ N, 50°06′11″ E).

2. Materials and Methods

2.1. Mechanical Design. The mechanical design of SAST and DAST is firstly made using a computer-aided design (CAD) software and underwent many enhancements and improvements to the mechanical structure of the trackers (as seen in Figure 1). The design had to be flexible enough to give

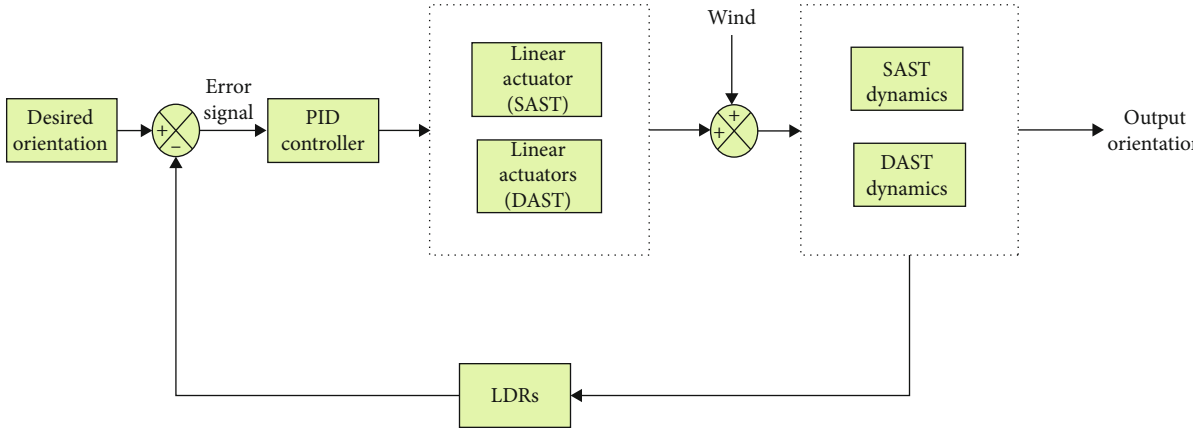

Figure 4: Block diagram of the close-loop feedback system.

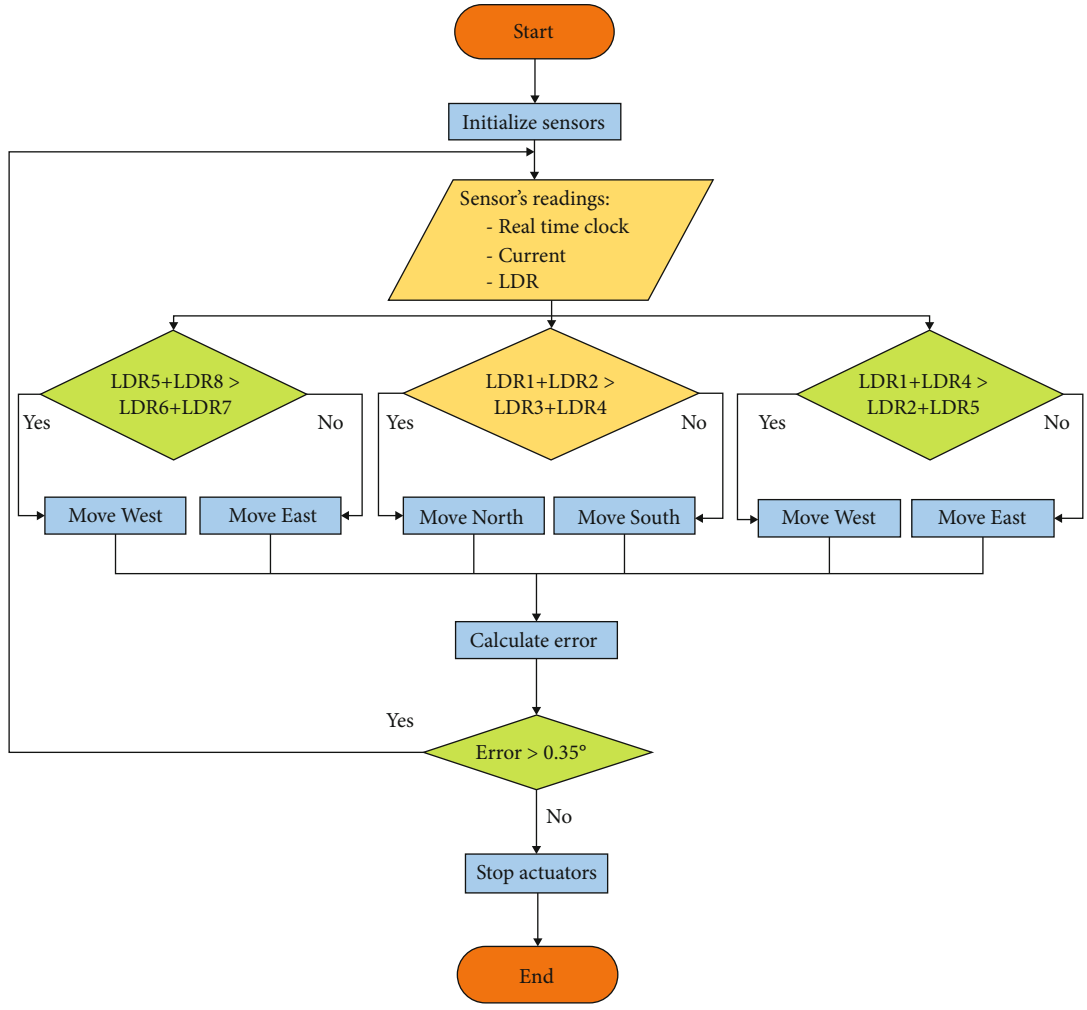

Figure 5: SAST and DAST working principle's flow chart.

effective degrees of freedom; in addition, it has to be stable under windy weather conditions or any other external disturbances. The actual models have been fabricated and manufactured in the mechanical workshop at Imam Abdulrahman Bin Faisal University (IAU).

2.2. Electrical Setup. To make the mechanical model of SAST and DAST functional, linear actuators have been integrated to give movement for the 50 W PV modules. The linear actuators receive signals via the motor drivers from an embedded controller (Arduino Mega) based on the light

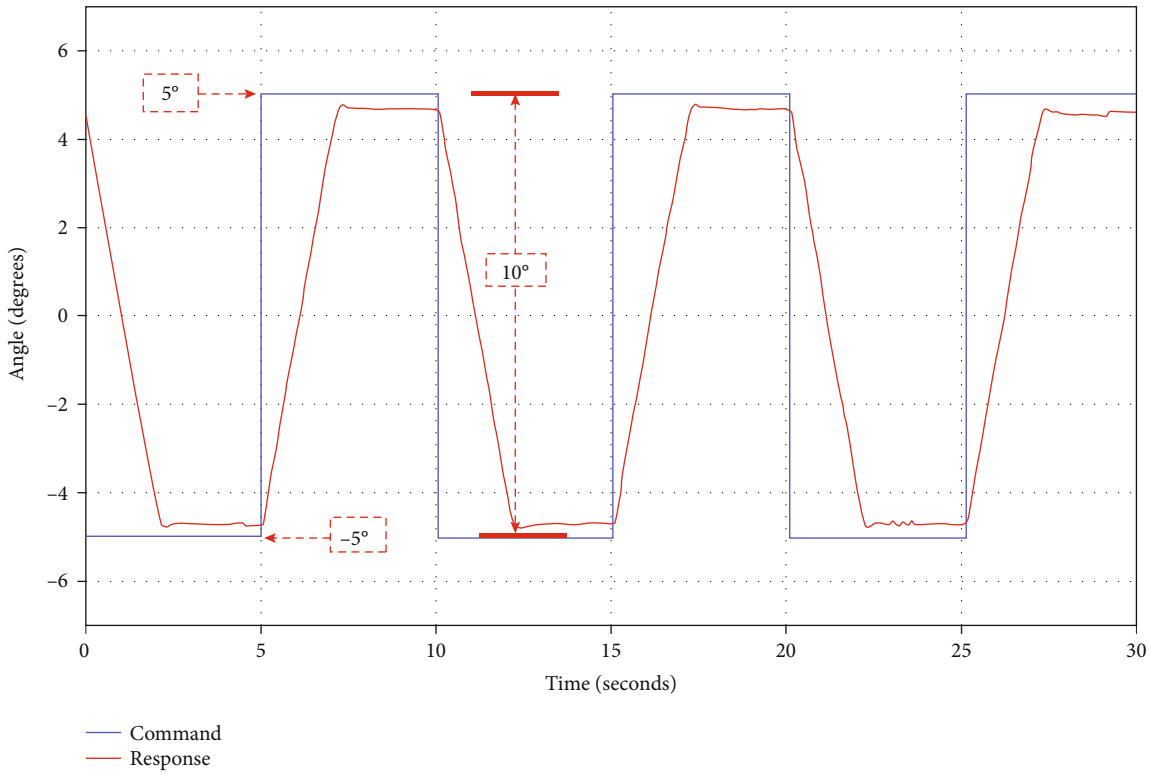

Figure 6: System's PID response.

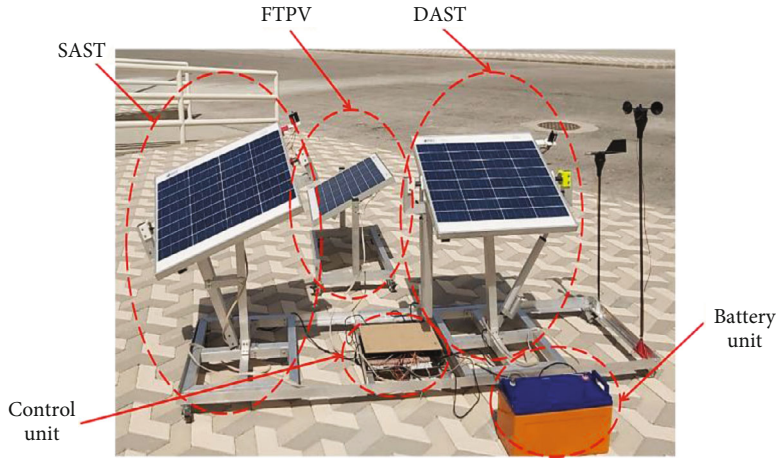

Figure 7: Experimental setup for FTPV, SAST, and DAST.

dependent resistor (LDR) readings. In addition to the electrical setup of SAST and DAST, an electrical set up for the measurement and acquisition of the sensors' signals has been constructed to achieve the goal of this experimental study as seen in Table 1 and Figures 2 and 3. The current measurements generated via each PV module have been recorded using a current sensor. At the same time, the currents consumed by each motor and the electrical control system have been measured using current sensors also. Furthermore, real-time-clock (RTC) has been used to give the time and date of the collected experimental data.

2.3. Control Schema. The controller used to manipulate the closed-loop system is a proportional integral derivative (PID) controller tuned experimentally to achieve an accurate, smooth, and power-friendly response based on equation (1). The STS under investigation has no input; instead, LDRs act as the sensors that provide the feedback signal to the PID controller upon which error calculations are made, following equation (2), equation (3), and equation (4), and orientation adjustments are decided (based on the highest intensity direction). After that, the microcontroller sends a signal to the actuators (linear motors) accordingly

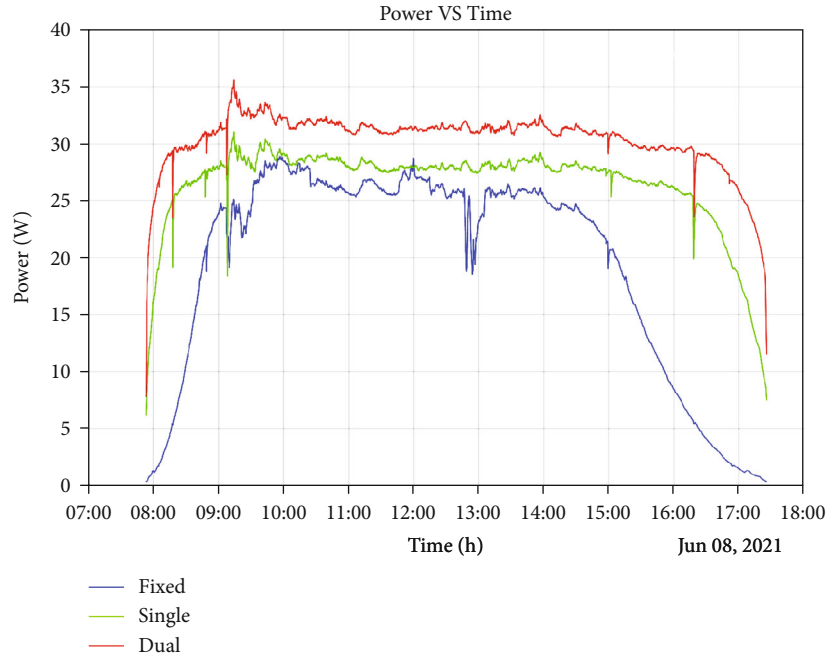

Figure 8: FTPV, SAST, and DAST power generation.

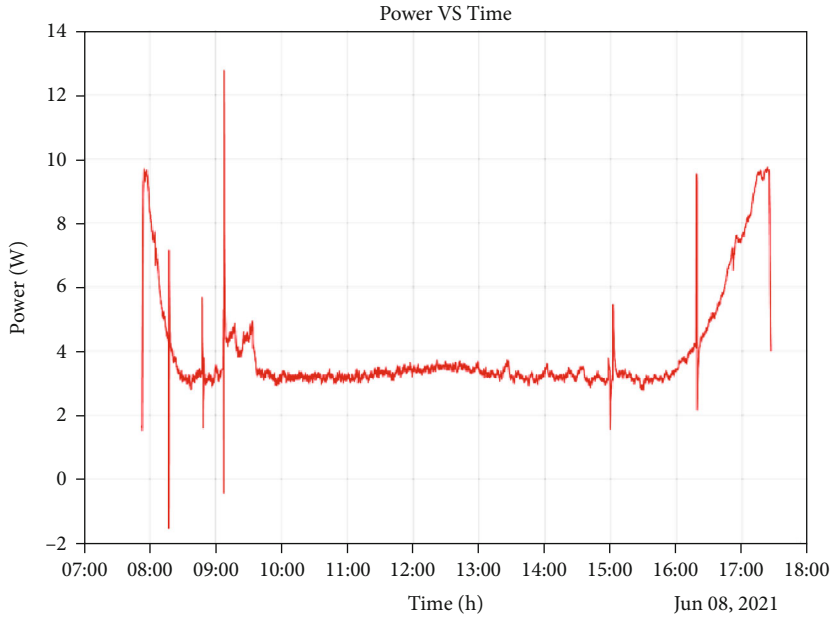

Figure 9: The difference in power generation between DAST and SAST.

(Figures 4 and 5).

$$\text{PID} = \left(K_p * E\right) + \left(K_i * iE\right) + \left(K_d * dE\right), \quad (1)$$

$$E = \text{CMD} - \text{feedback}, \quad (2)$$

$$iE = E * dt + iE\_\text{Prev}, \quad (3)$$

$$dE = \frac{E - E\_\text{Prev}}{dt}, \quad (4)$$

where K_p is the proportional component, E is the error, K_i is the integral component, E_i is the integral error, K_d is the derivative component, E_d is the derivative error, CMD is the command, and Prev is the previous.

2.4. Tracking System Resolution. An indoor experiment was implemented to determine the accuracy of the experiment's tracking systems. In this test, angles were given to the system as a command, and then, the actual tilt angles of the PV module were measured using an accelerometer sensor. After that, the actual angle measured was compared to the command given to the systems. Results of the resolution test

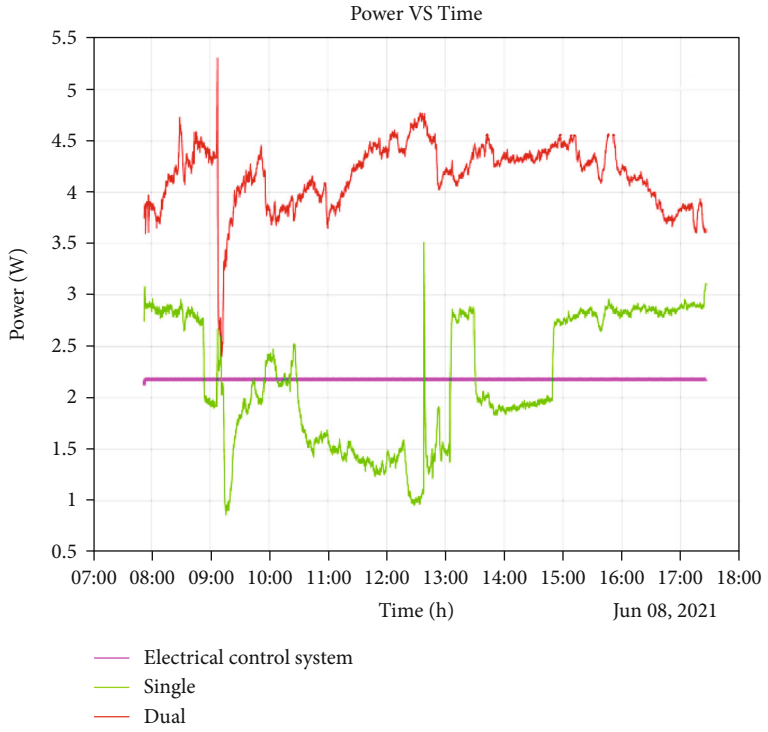

Figure 10: FTPV, SAST, and DAST power consumption.

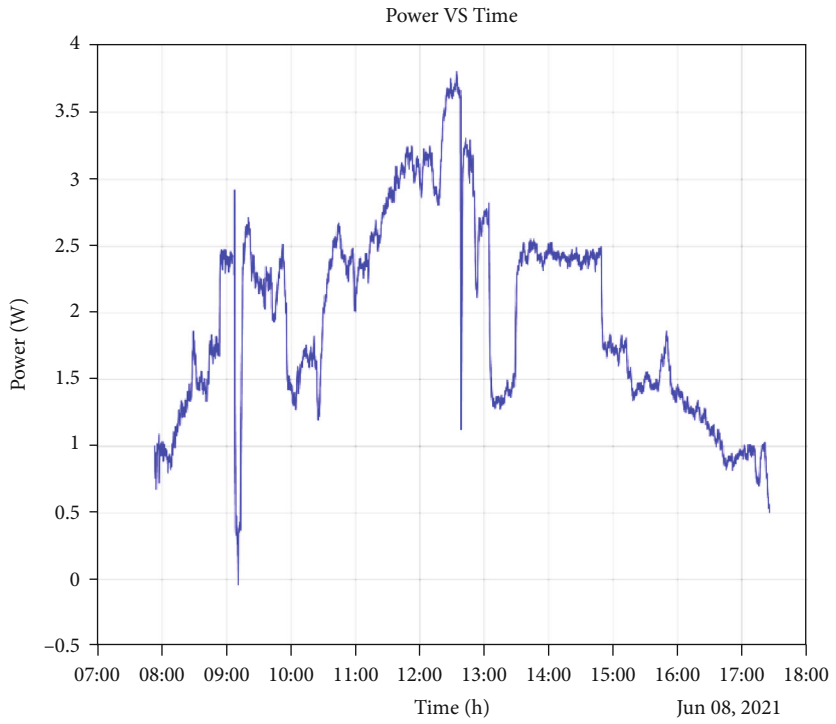

Figure 11: The difference in power consumption between DAST and SAST.

showed a high accuracy achieved by the developed tracking mechanism of about 0.35° as seen in Figure 6.

2.5. Experimental Procedure. The experiment presented in this study was conducted at IAU, in the city of Dammam, SA (26.4° latitude). The data is collected on June 8, 2021, on a sunny, clear day. To set up the experimental platforms for testing, the FTPV, single, and dual STS were placed and examined simultaneously to increase the reliability of the comparison as seen in Figure 7. The FTPV and SAST were

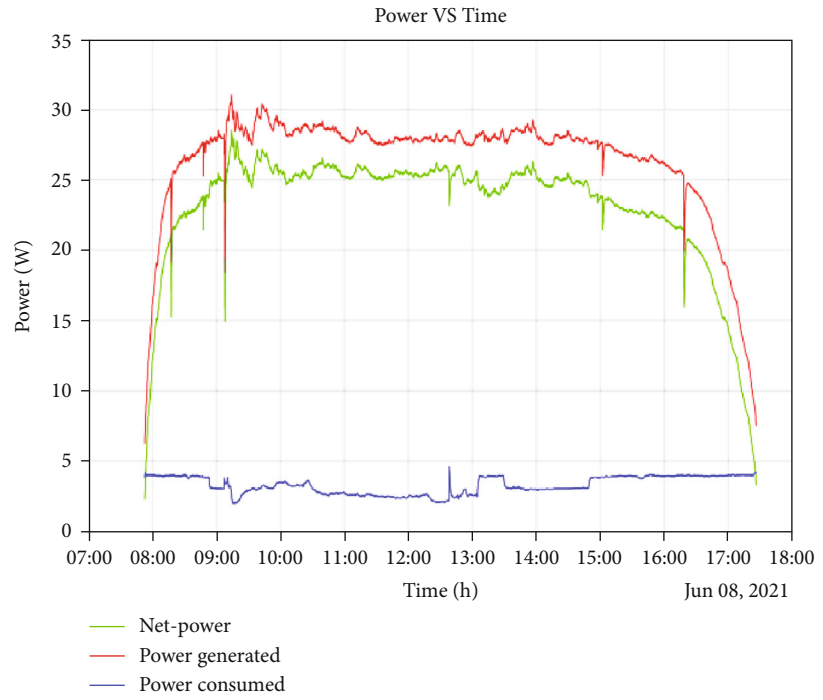

(a)

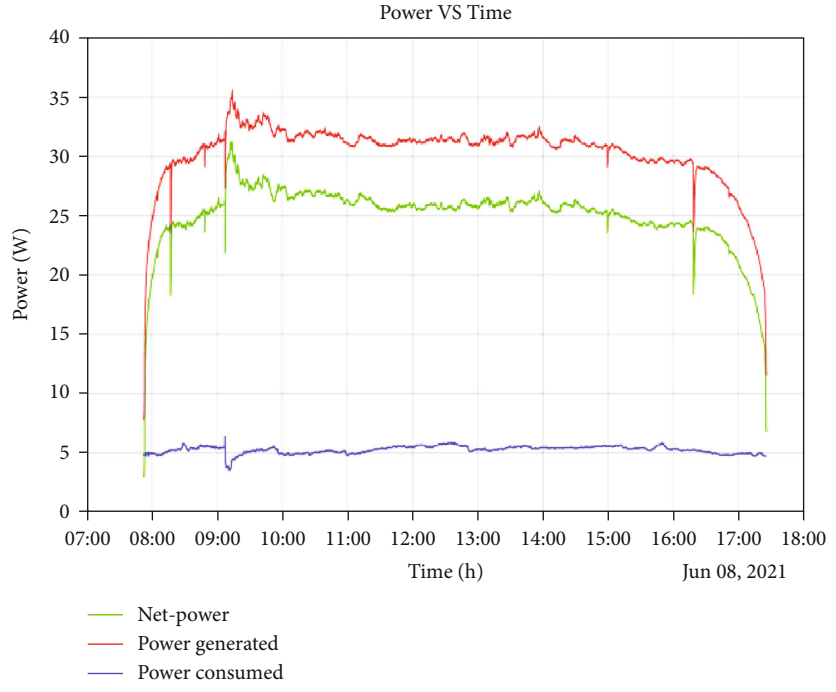

(b)

Figure 12: Continued.

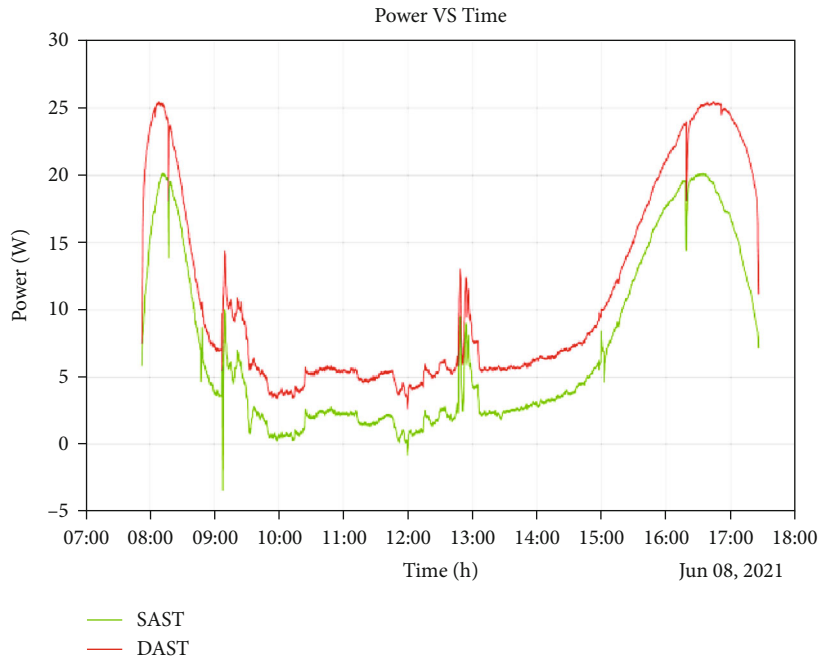

(c)

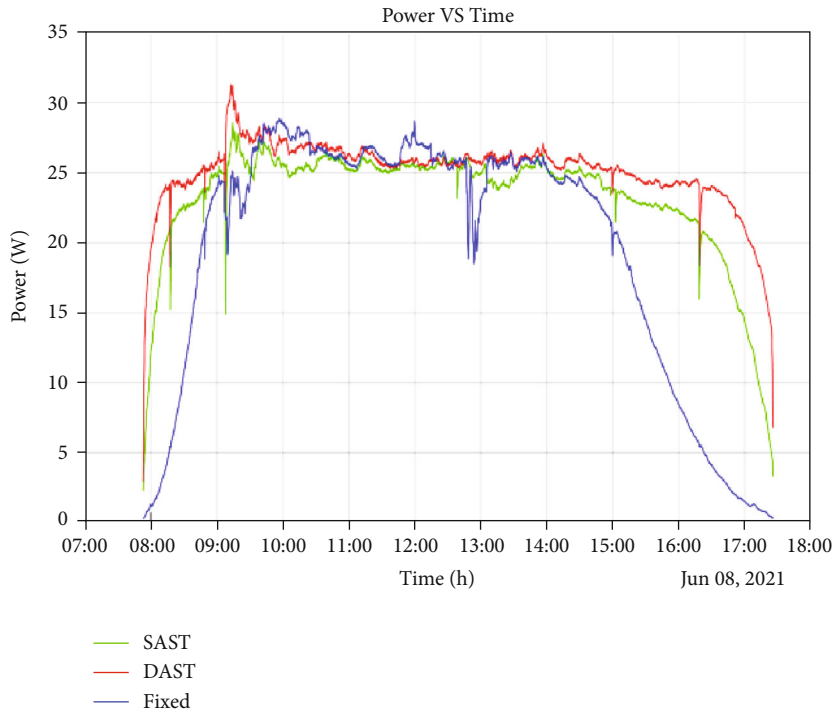

(d)

Figure 12: (a) Power generation, consumption, and the net power of SAST. (b) Power generation, consumption, and net power of DAST. (c) Increase in power (power improvement) of SAST and DAST. (d) Net power of SAST, DAST, and FTPV.

Table 2: Energy generated, consumed, and net energy via each system.

Energy generated (kJ)	
FTPV	398.6
SAST	536.3
DAST	615.4
Energy consumed (kJ)	
Electrical control system	42.3
SAST_actuator	42
DAST_actuators	80.2
Net energy (kJ)	
FTPV	398.6
SAST	473.2
DAST	514.1

initially oriented toward the optimal yearly tilt angle (OYTA) which is about 23°, since the latitude is between 25° and 50° and according to equation (5) [40]. In addition, as SA is located in the northern hemisphere, both FTPV and SAST were placed to face the south.

$$\text{OYTA} = (\text{latitude} * 0.76) + 3.1. \quad (5)$$

3. Results and Discussion

3.1. Power. The power production and consumption of FTPV, SAST, and DAST have been calculated throughout the day. The measurements for the power production of PV modules were recorded by utilizing the current measurements through power resistors acting as dummy-load (this strategy enables to measure the power without any voltage sensor), while the measurements of the power consumption through the actuators and the controllers were acquired via utilizing the current measurements with the known input voltage.

3.1.1. Power Production. The results of the power production showed expected outcomes since DAST showed the highest power production throughout the day. On the other hand, the FTPV showed the lowest power production, and the SAST power production was somewhere in between Figure 8. Furthermore, the power generation of SAST and DAST was almost the same at the beginning and the end of the experiment, while a significant difference occurred between these times. Also, the graph shows that the huge difference between FTPV and the PVTS is at the early and late hours of the day.

Figure 9 shows the difference in power generation between DAST and SAST. Remarkably, the highest difference in power generation occurs after the starting point by a few minutes as same as before the ending point by a few minutes. However, the average difference in power is about 3.9 W; although that seems low, the accumulation of this power with time leads to a high energy difference.

3.1.2. Power Consumption. In regard to power consumption, most papers claim that most of the power wasted is due to the actuators (motors) not the electrical system and that is what is studied in this section. The data collected from the experiment proved that the dominant power waste is due to the actuators (Figure 10) which is the same as what previous studies suggested.

The difference in power consumption between DAST and SAST, which is shown in Figure 11, proves that the difference in power consumption is not high (between 1 W and 3.5 W), although this slight difference leads to high energy consumption at the end of the day. Additionally, it is noticeable that the difference in power consumption starts to increase from the beginning and then starts to decrease after 12 : 30 approximately. And in terms of average value, the average difference of power consumption was about 2 W.

3.1.3. Net Power. To calculate the net power of SAST and DAST, the power produced by each system has been subtracted from the consumption of the motors and the electrical control system. Both SAST and DAST show positive net power as expected in Figures 12(a) and 12(b), which led to the understanding that both of these systems are beneficial. The increase in power (power improvement) of SAST and DAST was maximum at the beginning and the end of the test since the FTPV produced the lowest power in these times; however, it was minimum in the noon (Figure 12 (c)). In addition, the comparison between the net power of SAST, DAST, and FTPV shows similar results, since the net power of both SAST and DAST was maximum in comparison to FTPV at the beginning and end of the day (Figure 12(d)), while the net power was almost the same for all systems from 9 AM to 2 : 30 PM.

3.2. Energy. The energy can be calculated via taking the integration of any power VS time curve, and that was the approach to calculate the energy in this paper. Energy generated, consumed, and net energy of all systems are listed in Table 2. The energy generated from the FTPV was about 399 kJ, while SAST and DAST generate 34.6% and 54.4% more energy, respectively. On the other hand, the energy consumed via SAST is about 7.8% of its total generated energy, while DAST is about 13.0% of its total generated energy. Furthermore, the energy consumed from the SAST and the whole electrical control system was almost similar to each other, and the energy consumption for the DAST is almost equal to the sum of the energy consumed by both SAST and the control system, while the energy consumed via the electrical control system of SAST is about 3.9% of its total energy production, and the electrical control system of DAST consumed about 3.4% of its total energy production.

Most importantly, the increase in the net energy (INE) of SAST and DAST compared to FTPV has been calculated using equation (6). As a result, DAST achieves 28.98% INE while the SAST achieves 18.72% INE.

$$\text{INE} = (E_{\text{TS}} - (E_C + E_F)) * \frac{100}{E_F}, \quad (6)$$

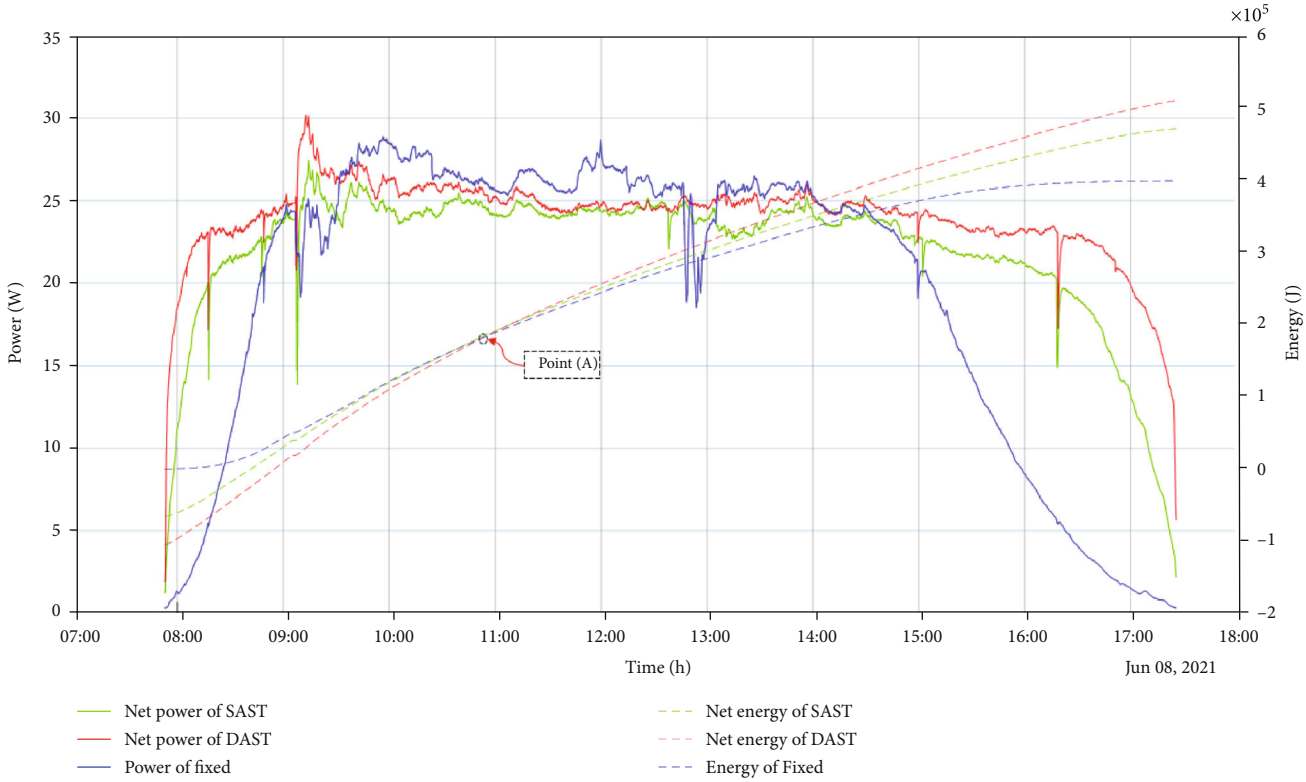

Figure 13: Net power and energy of SAST, DAST, and FTPV.

where INE is the increase in net energy of SAST or DAST, E_{TS} is the energy generated by SAST or DAST, E_F is the energy generated by FTPV, and E_C is the total energy consumed by SAST or DAST. Figure 13 shows the net power and energy of SAST, DAST, and FTPV. This graph is capable to show the power and the accumulation of energy throughout the day. A critical point in the energy curve is point (A) since the graph demonstrates that the net energy of each system from the highest to the lowest was as flows: FTPV, SAST, and DAST. In contrast after point (A), the graph shows the opposite order of net energy production.

The energy difference demonstrated at the beginning of the day between the FTPV, SAST, and DAST is due to the actuation mechanism compared to the production of the modules. After a few hours, the accumulation of energy for all three systems meets at point (A) (Figure 13) starting from which the DAST starts to have the most energy accumulation since it has the highest net power production. Also, the DAST has the highest power consumption since it has two actuators to adjust its orientation. Therefore, the energy curve of the DAST starts at the bottom and ends at the top. Additionally, point (A) clarifies that if DAST and SAST were exposed to the sun for an insufficient time (e.g., from 8 AM to 11 AM), both systems would be useless and cause negative INP.

4. Conclusion and Future Work

To sum up, in this study, the assembly and mechanization of single-axis and dual-axis microcontrolled PV tracking systems are demonstrated in order to determine the most efficient PV system for the region. Additionally, a unique investigation for the net energy generated and consumed by each system is carried out in the study.

The PVTS is actuated using linear motors and controlled via PID controllers in order to reorient 50 W PV modules to the direction of the sunlight. The algorithms of the PVTS were able to trace the sunlight with a resolution of 0.35°. The sheer amount of energy produced via the PVTS has recorded massive increases in comparison to the FTPV with an increase in energy production of 34.5% and 54.4% for SAST and DAST, respectively. However, after considering the power consumption of different components in the PVTS (the actuators and the electrical control setup), the net increase in energy is recorded to be about 18.72% and 28.98% for SAST and DAST, respectively, which demonstrates that DAST, SAST, and FTPV are the most efficient systems for the region, respectively. It is concluded that most of the energy consumption is due to the actuation mechanism, since SAST consumed about 7.8% of its total energy production, while DADT consumed 13.06% of its total energy production. The energy consumed by the electrical control system was 3.4% and 3.9% of the total energy production from SAST and DAST, respectively.

Although the result shows that DAST and SAST are compatible with the region in terms of increase in net energy, a financial analysis must be one to determine if the increase in energy production would cover the cost of manufacturing and maintenance, especially for DAST. Moreover, in order to further optimize the mechanical of the PVTS, a study of the wind profile should be made to investigate the effect of the wind force on the energy

consumption of the actuators. Furthermore, an investigation of various STS control algorithms on the consumption of the actuators should be carried out.

Abbreviations

PV: Solar photovoltaic
PVTS: Solar photovoltaic tracking system
FTPV: Fixed-tilt photovoltaic system
SAST: Single-axis solar tracking system
DAST: Dual-axis solar tracking system
STS: Solar tracking systems
CAD: Computer-aided design
LDR: Light dependent resistors
RTC: Real-time clock
Qty: Quantity
K_p: Proportional component
E: Error
K_i: Integral component
E_i: Integral error
K_d: Derivative component
E_d: Derivative error
CMD: Command
Prev: Previous.

Data Availability

The data used to support the findings of this study are included within the article, and references are described in the text of the article.

Conflicts of Interest

The authors declare that they have no known competing financial interests or personal relationships that could have appeared to influence the work reported in this paper.

Acknowledgments

The authors are grateful to the Deanship of Scientific Research (DSR) at Imam Abdulrahman bin Faisal University, Kingdom of Saudi Arabia, for their continuous guidance and support.

References

[1] S. Mubaarak, D. Zhang, Y. Chen et al., "Techno-economic analysis of grid-connected PV and fuel cell hybrid system using different PV tracking techniques," *Applied Sciences*, vol. 10, no. 23, p. 8515, 2020.

[2] M. S. Shaari, Z. Abdul Karim, and N. Zainol Abidin, "The effects of energy consumption and national output on CO2 emissions: new evidence from OIC countries using a panel ARDL analysis," *Sustainability*, vol. 12, no. 8, p. 3312, 2020.

[3] F. J. Gómez-Uceda, J. Ramirez-Faz, M. Varo-Martinez, and L. M. Fernández-Ahumada, "New omnidirectional sensor based on open-source software and hardware for tracking and backtracking of dual-axis solar trackers in photovoltaic plants," *Sensors*, vol. 21, no. 3, p. 726, 2021.

[4] M. I. Hussain and J.-T. Kim, "Performance evaluation of photovoltaic/thermal (PV/T) system using different design configurations," *Sustainability*, vol. 12, no. 22, p. 9520, 2020.

[5] F. M. Mustafa, "Dual-axis solar tracking over fixed solar systems," *International Journal of Advances in Engineering and Technology*, vol. 9, no. 5, p. 563, 2016.

[6] C. Alexandru, "Optimization of the bi-axial tracking system for a photovoltaic platform," *Energies*, vol. 14, no. 3, p. 535, 2021.

[7] H. Zsiborács, A. Bai, J. Popp et al., "Change of real and simulated energy production of certain photovoltaic technologies in relation to orientation," *Sustainability*, vol. 10, no. 5, p. 1394, 2018.

[8] J. Siecker, K. Kusakana, and B. P. Numbi, "A review of solar photovoltaic systems cooling technologies," *Renewable & Sustainable Energy Reviews*, vol. 79, pp. 192–203, 2017.

[9] S. Seme, B. Štumberger, M. Hadžiselimović, and K. Sredenšek, "Solar photovoltaic tracking systems for electricity generation: a review," *Energies*, vol. 13, no. 16, p. 4224, 2020.

[10] S. Das, S. Chakraborty, P. K. Sadhu, and O. S. Sastry, "Design and experimental execution of a microcontroller (μC)-based smart dual- axis automatic solar tracking system," *Energy Science & Engineering*, vol. 3, no. 6, pp. 558–564, 2015.

[11] R. J. Mustafa, M. R. Gomaa, M. Al-Dhaifallah, and H. Rezk, "Environmental impacts on the performance of solar photovoltaic systems," *Sustainability*, vol. 12, no. 2, p. 608, 2020.

[12] A. Masih and I. Odinaev, "Performance Comparison of Dual Axis Solar Tracker with Static Solar System in Ural Region of Russia," in *2019 Ural Symposium on Biomedical Engineering, Radioelectronics and Information Technology (USBEREIT)*, pp. 375–378, Yekaterinburg, Russia, 2019.

[13] A. E. Hammoumi, S. Motahhir, A. E. Ghzizal, A. Chalh, and A. Derouich, "A simple and low-cost active dual-axis solar tracker," *Energy Science & Engineering*, vol. 6, no. 5, pp. 607–620, 2018.

[14] W. Nsengiyumva, S. G. Chen, L. Hu, and X. Chen, "Recent advancements and challenges in solar tracking systems (STS): a review," *Renewable & Sustainable Energy Reviews*, vol. 81, pp. 250–279, 2018.

[15] F. Grubišić-Čabo, S. Nižetić, I. Marinić Kragić, and D. Čoko, "Further progress in the research of fin-based passive cooling technique for the free-standing silicon photovoltaic panels," *International Journal of Energy Research*, vol. 43, no. 8, pp. 3475–3495, 2019.

[16] S. A. S. Eldin, M. S. Abd-Elhady, and H. A. Kandil, "Feasibility of solar tracking systems for PV panels in hot and cold regions," *Renewable Energy*, vol. 85, pp. 228–233, 2016.

[17] S. Racharla and K. Rajan, "Solar tracking system - a review," *International Journal of Sustainable Engineering*, vol. 10, no. 2, pp. 72–81, 2017.

[18] M. N. A. M. Said, S. A. Jumaat, and C. R. A. Jawa, "Dual axis solar tracker with IoT monitoring system using arduino," *International Journal of Power Electronics and Drive Systems*, vol. 11, no. 1, p. 451, 2020.

[19] A. Z. Hafez, A. M. Yousef, and N. M. Harag, "Solar tracking systems: technologies and trackers drive types - a review," *Renewable & Sustainable Energy Reviews*, vol. 91, pp. 754–782, 2018.

[20] S. Gutierrez, P. M. Rodrigo, J. Alvarez, A. Acero, and A. Montoya, "Development and testing of a single-axis photovoltaic sun tracker through the Internet of Things," *Energies*, vol. 13, no. 10, p. 2547, 2020.

[21] N. Al-Rousan, N. A. M. Isa, and M. K. M. Desa, "Advances in solar photovoltaic tracking systems: a review," *Renewable & Sustainable Energy Reviews*, vol. 82, pp. 2548–2569, 2018.

[22] J. da Rocha Queiroz, A. da Silva Souza, M. K. Gussoli, J. C. D. de Oliveira, and C. M. G. Andrade, "Construction and automation of a microcontrolled solar tracker," *Processes*, vol. 8, no. 1309, 2020.

[23] A. J. Farhan, "Fabrication and development low cost dual axis solar tracking system," *Materials Science and Engineering*, vol. 757, no. 1, article 012042, 2020.

[24] R. F. Fuentes-Morales, A. Diaz-Ponce, M. I. Peña-Cruz et al., "Control algorithms applied to active solar tracking systems: a review," *Solar Energy*, vol. 212, pp. 203–219, 2020.

[25] D. Mazumdar, D. Sinha, S. Panja, and D. K. Dhak, "Design of LQR controller for solar tracking system," in *2015 IEEE International Conference on Electrical, Computer and Communication Technologies (ICECCT)*, pp. 1–5, Coimbatore, India, 2015.

[26] T. Laseinde and D. Ramere, "Low-cost automatic multi-axis solar tracking system for performance improvement in vertical support solar panels using Arduino board," *International Journal of Low Carbon Technologies*, vol. 14, no. 1, pp. 76–82, 2019.

[27] Q. Li and M. E. Baran, "A novel frequency support control method for PV plants using tracking LQR," *IEEE Transactions on Sustainable Energy*, vol. 11, no. 4, pp. 2263–2273, 2020.

[28] A. Rawat, S. K. Jha, and B. Kumar, "Position controlling of sun tracking system using optimization technique," *Energy Reports*, vol. 6, pp. 304–309, 2020.

[29] N. Arab, B. Kedjar, A. Javadi, and K. Al-Haddad, "A multifunctional single-phase grid-integrated residential solar PV systems based on LQR control," *IEEE Transactions on Industry Applications*, vol. 55, no. 2, pp. 2099–2109, 2019.

[30] X. Du, Y. Li, P. Wang, Z. Ma, D. Li, and C. Wu, "Design and optimization of solar tracker with U-PRU-PUS parallel mechanism," *Mechanism and Machine Theory*, vol. 155, article 104107, 2021.

[31] X. C. Ngo, T. H. Nguyen, N. Y. Do et al., "Grid-connected photovoltaic systems with single-axis sun tracker: case study for Central Vietnam," *Energies*, vol. 13, no. 6, p. 1457, 2020.

[32] J. Ruelas, F. Muñoz, B. Lucero, and J. Palomares, "PV tracking design methodology based on an orientation efficiency chart," *Applied Sciences*, vol. 9, no. 5, p. 894, 2019.

[33] H. Z. Al Garni, A. Awasthi, and M. A. M. Ramli, "Optimal design and analysis of grid-connected photovoltaic under different tracking systems using HOMER," *Energy Conversion and Management*, vol. 155, pp. 42–57, 2018.

[34] A. F. Almarshoud, "Performance of solar resources in Saudi Arabia," *Renewable and Sustainable Energy Reviews*, vol. 66, pp. 694–701, 2016.

[35] A. Alrashidi, *Investigating the Feasibility of Solar Photovoltaic Systems in Kuwait, [Ph.D]*, Loughborough University, 2017.

[36] M. Ghassoul, "Single axis automatic tracking system based on PILOT scheme to control the solar panel to optimize solar energy extraction," *Energy Reports*, vol. 4, pp. 520–527, 2018.

[37] F. F. Ahmad, M. Abdelsalam, A. K. Hamid, C. Ghenai, W. Obaid, and M. Bettayeb, "Experimental Validation of PVSYST Simulation for Fix Oriented and Azimuth Tracking Solar PV System," in *International Conference on Modelling, Simulation and Intelligent Computing*, N. Goel, S. Hasan, and V. Kalaichelvi, Eds., vol. 659 of Lecture Notes in Electrical Engineering, pp. 227–235, Springer, Singapore, 2020.

[38] N. Al Safarini, O. Akash, M. Mohsen, and Z. Iqbal, "Performance evaluation of solar tracking systems for power generation based on simulation analysis: solar island concept," in *2017 International Conference on Electrical and Computing Technologies and Applications (ICECTA)*, pp. 1–4, Ras Al Khaimah, United Arab Emirates, 2017.

[39] M. E. H. Chowdhury, A. Khandakar, B. Hossain, and R. Abouhasera, "A low-cost closed-loop solar tracking system based on the sun position algorithm," *Journal of Sensors*, vol. 2019, Article ID 3681031, 11 pages, 2019.

[40] D. Torres and J. Crichigno, "Influence of reflectivity and cloud cover on the optimal tiltangle of solar panels," *Resources (Basel)*, vol. 4, no. 4, pp. 736–750, 2015.